PAPER

NJC
www.rsc.org/njc

Pyridylporphyrins peripherally coordinated to ruthenium-nitrosyls, including the water-soluble $Na_4[Zn \cdot 4'TPyP\{RuCl_4(NO)\}_4]$: synthesis and structural characterization†

Teresa Gianferrara,[a] Barbara Serli,[b] Ennio Zangrando,[b] Elisabetta Iengo[b] and Enzo Alessio*[b]

[a] *Dipartimento di Scienze Farmaceutiche, Università di Trieste, Piazzale Europa 1, 34127 Trieste, Italy. E-mail: gianfer@univ.trieste.it; Fax: +39 040 52572; Tel: +39 040 5587859*

[b] *Dipartimento di Scienze Chimiche, Università di Trieste, Via Giorgieri 1, 34127 Trieste, Italy. E-mail: alessi@univ.trieste.it; Fax: +39 040 5583903; Tel: +39 040 5583961*

Received (in Montpellier, France) 15th December 2004, Accepted 11th March 2005
First published as an Advance Article on the web 13th May 2005

Several new ruthenium-nitrosyl conjugates with *meso*-4′pyridylporphyrins, namely the two anionic isomers $[n\text{Bu}_4\text{N}][trans\text{-RuCl}_4(4'\text{MPyP})(\text{NO})]$ (**1**) and $[n\text{Bu}_4\text{N}][cis\text{-RuCl}_4(4'\text{MPyP})(\text{NO})]$ (**2**), the two neutral isomers $[mer,trans\text{-RuCl}_3(4'\text{MPyP})_2(\text{NO})]$ (**3**) and $[mer,cis\text{-RuCl}_3(4'\text{MPyP})_2(\text{NO})]$ (**4**), and the tetraruthenated adduct $[n\text{Bu}_4\text{N}]_4[4'\text{TPyP}\{\text{RuCl}_4(\text{NO})\}_4]$ (**5**) were obtained by reaction of $[n\text{Bu}_4\text{N}][trans\text{-RuCl}_4(\text{dmso-O})(\text{NO})]$ with 4′MPyP and 4′TPyP (*meso*-4′monopyridylporphyrin and *meso*-4′tetrapyridylporphyrin, respectively). The X-ray structures of **2**, **4**, and **5** are described. Exchange of $n\text{Bu}_4\text{N}^+$ for Na^+ eventually led to the water-soluble tetraruthenated porphyrin $\text{Na}_4[\text{Zn} \cdot 4'\text{TPyP}\{\text{RuCl}_4(\text{NO})\}_4]$ (**6 · Zn**).

Introduction

Synthetic water-soluble porphyrins and metalloporphyrins, including cationic, anionic and sugar-substituted types, are of considerable interest for their potential biological and biomedical applications. In fact, besides as photosynthetic models,[1] they have been extensively investigated in several bio-related fields, such as: (i) specific DNA binding *via* intercalation and/or outside association,[2] including interactions with quadruplex DNA and telomerase inhibition;[3,4] (ii) chemical or photochemical induced DNA cleavage;[5] (iii) photodynamic therapy for the treatment of cancer,[6]‡ exploiting the preferential uptake and retention of the porphyrins by tumor tissues;[7] (iv) antiviral activity (including anti HIV-1)[8] (v) anticancer activity,[9] including boron neutron capture therapy of tumors (porphyrins labelled with boron compounds);[10] and (vi) acetylcholinesterase inhibition.[11] In addition, water-soluble porphyrins have been investigated as: (i) models of the iron hemoproteins;[12] (ii) contrast agents for MRI [porphyrins labelled with paramagnetic metal centers, such as Fe(III) or Mn(III)],[13] for fluorescence,[14] and for radiological imaging (porphyrins labelled with radioactive metal centers);[15] (iii) biomimetic models for the metabolic bio-oxidation of drugs and DNA;[16] (iv) hypoxic agents, especially as cytotoxins and radiosensitizers (in particular when bringing nitro or nitroso functionalities);[17] and (v) artificial peptide receptors.[18]

The most commonly used strategies for obtaining water-soluble synthetic porphyrins involve the attachment of either hydrophilic or easily ionizable (or altogether charged) functional groups to the periphery of the chromophore, mainly at the *meso* positions. Cationic porphyrins are commonly derived from *meso*-tetra(aminophenyl)porphyrin or from *meso*-tetrapyridylporphyrin by protonation of the amino groups or alkylation of the pyridyl groups, respectively [*e.g.* tetra(*p*-*N*-methylpyridyl)porphyrin]. Phosphonium and ammonium cationic porphyrins have also been described.[19] Anionic porphyrins are prepared by attachment of –OH, –COOH, or $–SO_3Na$ functions to the aryl groups in *meso*-tetraarylporphyrins [most commonly tetraphenylporphyrin, *e.g.*, the widely used tetra(*p*-carboxyphenyl)porphyrin and tetra(*p*-sulfonatophenyl)porphyrin].

An intriguing alternative to the above synthetic strategies is that of coordinating water-soluble (*e.g.*, charged) metal complexes to peripheral sites of the porphyrins. Besides solubilizing the porphyrin, such fragments would influence its steric requirements and might introduce further useful functionalities into the system. For example, Brunner and co-workers prepared porphyrin-platinum conjugates with the aim of combining the cytostatic effect of the platinum fragment and (upon irradiation) the phototoxic effect of the porphyrin sensitizer.[20] In addition, water-soluble porphyrin-Pt(II) conjugates are expected to have a greater tumor selectivity as compared to platinum compounds, by virtue of the accumulation of porphyrins in malignant tissues (tumor-targeting properties).[21] The other examples of this kind found in the literature mainly concern the symmetrical coordination of the peripheral N atoms of *meso*-4′tetrapyridylporphyrin (4′TPyP or metallated 4′TPyP) to a number of charged metal fragments, such as: $[Ru(NH_3)_5]^{2+}$,[22] $[Ru(bpy)_2Cl]^+$, $[Ru(phen)_2Cl]^+$, or $[Ru(EDTA)]^-$,[23] $[RuCl_4(dmso\text{-}S)]^-$ or $[RuCl_4(CO)]^-$,[24] $[Fe(CN)_5]^-$,[25] $[Pt(Lau_2dim)(CH_3)]^+$ (Lau_2dim = didodecyldiimine),[26] and the hexotic hexanuclear rhenium-selenide cluster $[Re_6(\mu\text{-Se})_8(PEt)_5(MeCN)]^{2+}$.[27] $[Zn \cdot 4'TPyP\{Ru(bpy)_2Cl\}_4]^+$ was found to promote the photocatalytic oxidation of calf thymus DNA.[28] However, not all these charged porphyrins were found to be soluble in water, their solubility depending both on the nature of the ligands on the metal fragments and

† Electronic supplementary information (ESI) available: ^{1}H NMR spectra of compounds **1** and **2** ($CDCl_3$), **5** (CD_3NO_2), and **6Zn** (CD_3OD); perspective view of the solid state structure of **4**; ES-MS and MS-MS spectrum of **6Zn**. See http://www.rsc.org/suppdata/nj/b4/b418855a/.

‡ The porphyrins act as photosensitizers and the singlet oxygen that is formed upon irradiation kills the cells.

DOI: 10.1039/b418855a

on the nature of the counter-ions; for example, [4′TPyP{Pt(Lau$_2$dim)(CH$_3$)}$_4$](CF$_3$SO$_3$)$_4$ is insoluble in water but soluble in micellar phases,[29] and [*n*Bu$_4$N]$_4$[4′TPyP{RuCl$_4$(dmso-S)}$_4$] is soluble in chloroform and dmso, but not in water.[24]

We have a considerable experience in the use of pyridylporphyrins for the construction of metal-mediated supramolecular assemblies[30] and, recently, we synthesized a series of Ru-dmso nitrosyls of general formula [Ru(dmso-O)$_x$Cl$_{5-x}$(NO)]$^{(x-2)}$ (x = 1–5) and investigated their reactivity.[31] In particular, the anionic member of the series, [*trans*-RuCl$_4$(dmso-O)(NO)]$^-$, was found to replace selectively the O-bonded dmso with heterocyclic N-donors (L), yielding complexes of the type [RuCl$_4$(L)(NO)]$^-$; these products, which are quite stable and inert, may have either a cis or trans geometry, depending on the nature of L and the synthetic conditions. Thus, [*trans*-RuCl$_4$(dmso-O)(NO)]$^-$ seemed a good candidate to be used as precursor for appending charged [RuCl$_4$(NO)]$^-$ fragments to the peripheral N-atoms of pyridylporphyrins, with the final aim of obtaining water-soluble products. The presence of the nitrosyl group on the peripheral fragments introduces some further advantages: (i) NO is a good reporter group, as its stretching mode gives a strong infrared absorption band that is also quite sensitive to the nature of the trans-coordinated ligand and (ii) porphyrins bearing nitrosyl complexes might be investigated as controlled NO-releasing agents. Indeed, thermally stable ruthenium-nitrosyl complexes that might selectively release NO through redox or photochemical activation for medicinal purposes have attracted considerable interests.[32] We demonstrated that mono-electronic reduction of [Ru(dmso-O)$_x$Cl$_{5-x}$(NO)]$^{(x-2)}$ complexes and of their derivatives with heterocyclic N-donors induces the rapid release of NO.[31] Light absorption by the porphyrin chromophore might facilitate the photodissociation of NO (coordinated to the same metal center), as a consequence of photo-induced electron transfer.[33]

We report here a detailed investigation of the reactivity of [*n*Bu$_4$N][*trans*-RuCl$_4$(dmso-O)(NO)] towards 4′MPyP (*meso*-5-4′pyridyl-10,15,20-triphenylporphyrin) and 4′TPyP,§ that led to the isolation and structural characterization of several new porphyrin-ruthenium-nitrosyl conjugates, including the water-soluble Na$_4$[Zn·4′TPyP{RuCl$_4$(NO)}$_4$].

Experimental

Instrumentation

Infrared spectra (KBr) were obtained on a Perkin–Elmer 2000 NIR FT-Raman spectrometer. The IR spectra in solution were recorded in cells with BaF$_2$ (D$_2$O) or NaCl (CH$_3$NO$_2$) windows. ^{1}H NMR spectra were collected at 400 MHz on a Jeol Eclipse 400 FT spectrometer, with 2,2-dimethyl-2,2-silapentane-5-sulfonate (DSS) as an internal standard for D$_2$O solutions and residual non-deuterated solvent signal as reference for acetone-d_6 (δ = 2.04), CD$_3$NO$_2$ (δ = 4.33), CD$_3$OD (δ = 3.30), and CDCl$_3$ (δ = 7.26) spectra. Spectra were recorded at room temperature, unless differently specified. The labelling scheme of porphyrin protons is reported in Fig. 1 below. UV-Vis spectra were obtained on a Jasco V-550 spectrometer in quartz cells (path length 0.1, 1, or 10 mm). Mass spectra were collected on a ThermoFinnigan LCQ™ DecaXP Plus quadrupole ion trap instrument; the spray voltage was set at 5 kV and the capillary temperature at 50 °C.[34] Elemental analyses were performed at the Dipartimento di Scienze Chimiche, University of Trieste. *meso*-4′Pyridylporphyrins (4′MPyP and 4′TPyP) and the complex [*n*Bu$_4$N][*trans*-RuCl$_4$(dmso-O)(NO)] were prepared and purified as previously described.[30,31]

§ [*n*Bu$_4$N][*trans*-RuCl$_4$(dmso-O)(NO)] is quite soluble in most organic solvents, including CHCl$_3$ and CH$_2$Cl$_2$, the only solvents in which 4′TPyP is also slightly soluble.

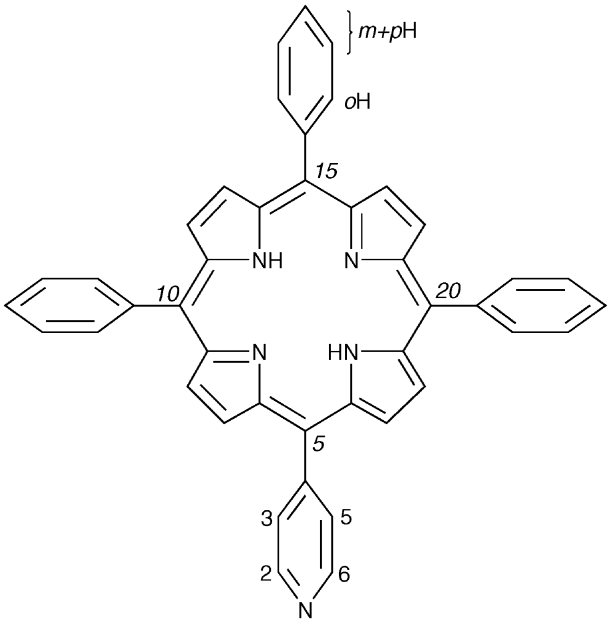

Fig. 1 Schematic drawing of *meso*-5-4′pyridyl-*10*,*15*,*20*-triphenylporphyrin (4′MPyP) with labelling scheme.

Column chromatography was performed using silica gel 60 Å, 230–400 mesh.

Synthesis of the complexes

[*n*Bu$_4$N][*trans*-RuCl$_4$(4′MPyP)(NO)] (1) and [*n*Bu$_4$N][*cis*-RuCl$_4$(4′MPyP)(NO)] (2). A 0.11 g amount of 4′MPyP (0.16 mmol) was added to 0.1 g of [*n*Bu$_4$N][*trans*-RuCl$_4$(dmso-O)(NO)] (0.16 mmol) dissolved in 25 ml of dichloromethane; the solution was refluxed for 72 h. According to TLC analysis (silica gel, CH$_3$CN–CHCl$_3$ 1 : 1), a mixture of two major products, **1** and **2** (besides some unbound 4′MPyP), was obtained. Column chromatography of the raw product on silica gel, eluting with a CHCl$_3$–CH$_3$CN mixture (9 : 1) afforded, in this order, pure **1** (12%) and **2** (30%). Very similar results were obtained running the reaction in chloroform at 40 °C for 72 h.

[*n*Bu$_4$N][*trans*-RuCl$_4$(4′MPyP)(NO)]·0.5CHCl$_3$ (1). The product from the column (first band) was recrystallized from chloroform–*n*-hexane; yield 20 mg (12%). R_f = 0.82 (silica gel, CH$_3$CN–CHCl$_3$ 1 : 1). Anal. calcd for C$_{59}$H$_{65}$N$_7$Cl$_4$ORu·0.5CHCl$_3$ (M_W): C, 60.0; H, 5.54; N, 8.23; found: C, 58.5; H, 5.62; N, 8.27. ^{1}H-NMR (CDCl$_3$, ppm): 9.85 (d, 2, H2,6), 8.90, 8.85 (m, 8, Hβ), 8.25 (d, 2, H3,5), 8.21 (m, 6, *o*-H), 7.77 (m, 9, *m* + *p*-H), 3.40 (m, 8, *n*Bu$_4$N$^+$), 1.75 (m, 8, *n*Bu$_4$N$^+$), 1.58 (m, 8, *n*Bu$_4$N$^+$), 1.07 (t, 12, *n*Bu$_4$N$^+$), −2.81 (s, 2, NH). Selected IR (KBr, cm^{-1}): 1872 (vs, $\nu_{N\equiv O}$), 334 (s, ν_{Ru-Cl}). UV-Vis (CHCl$_3$, T = 25 °C) λ_{max}/nm ($\varepsilon \times 10^{-3}$/dm^3 mol^{-1} cm^{-1}): 421 (311), 517 (17.6), 553 (9.7), 589 (6.9), 645 (5.5).

[*n*Bu$_4$N][*cis*-RuCl$_4$(4′MPyP)(NO)]·2CHCl$_3$ (2). This product was eluted in the second band and was recrystallized from chloroform–*n*-hexane; yield 50 mg (30%). R_f = 0.60 (silica gel, CH$_3$CN–CHCl$_3$ 1 : 1). Anal. calcd for C$_{59}$H$_{65}$N$_7$Cl$_4$ORu·2CHCl$_3$ (M_W 1369.84): C, 53.5; H, 4.68; N, 7.16; found: C, 51.5; H, 4.68; N, 7.03. ^{1}H-NMR (CDCl$_3$, ppm): 9.59 (d, 2, H2,6), 8.93, 8.87 (m, 8, Hβ), 8.27 (d, 2, H3,5), 8.21 (m, 6, *o*-H), 7.77 (m, 9, *m* + *p*-H), 3.40 (m, 8, *n*Bu$_4$N$^+$), 1.75 (m, 8, *n*Bu$_4$N$^+$), 1.58 (m, 8, *n*Bu$_4$N$^+$), 1.07 (t, 12, *n*Bu$_4$N$^+$), −2.79 (s, 2, NH). Selected IR (KBr, cm^{-1}): 1851 (s, $\nu_{N\equiv O}$), 331, 320 (m, ν_{Ru-Cl}). UV-Vis (CHCl$_3$, T = 25 °C) λ_{max}/nm ($\varepsilon \times 10^{-3}$/dm^3 mol^{-1} cm^{-1}): 421 (387), 516 (20.2), 551

(10.6), 590 (7.5), 645 (6.2). Crystals suitable for X-ray diffraction were obtained by slow diffusion of *n*-hexane into a chloroform solution of **2**.

[*n*Bu$_4$N][*cis*-RuCl$_4$(4′MPyP)(NO)] (2), [RuCl$_3$(4′MPyP)$_2$(NO)] (3), and [*mer*,*cis*-RuCl$_3$(4′MPyP)$_2$(NO)] (4). A 0.17 g amount of 4′MPyP (0.25 mmol) was added to 0.15 g of [*n*Bu$_4$N][*trans*-RuCl$_4$(dmso-O)(NO)] (0.25 mmol) dissolved in 20 ml of chloroform; the solution was refluxed for 2 h. According to TLC analysis (silica gel, $CHCl_3$), a mixture of three major products, **2–4** (besides some unbound 4′MPyP), was obtained. They were separated by column chromatography on silica gel; elution with $CHCl_3$ afforded, in the order: **3**, **4**, and 4′MPyP. An increase of the solvent polarity ($CHCl_3$–EtOH 9 : 1 mixture) afforded compound **2** (43%).

[RuCl$_3$(4′MPyP)$_2$(NO)] (3). The product was recrystallized from chloroform–*n*-hexane. R_f = 0.95 (silica gel, $CHCl_3$). Yield: 70 mg (17%). Anal. calcd for $C_{86}H_{58}N_{11}Cl_3ORu \cdot CHCl_3$ (M_W 1588.28): C, 65.8; H, 3.74; N, 9.70; found: C, 64.9; H, 3.60; N, 9.18. ^{1}H-NMR ($CDCl_3$, ppm): 9.75 (d, 4, H2,6), 8.99 (d, 4, Hβ), 8.96 (d, 4, Hβ), 8.88 (m, 8, Hβ), 8.48 (d, 4, H3,5), 8.24 (m, 12, *o*-H), 7.80 (m, 18, *m* + *p*-H), −2.75 (s, 4, NH). Selected IR (KBr, cm^{-1}): 1861 (s, $\nu_{N\equiv O}$). UV-Vis ($CHCl_3$, T = 25 °C) λ_{max}/nm (ε × 10^{-3}/dm^3 mol^{-1} cm^{-1}): 422 (648), 517 (38.8), 554 (22.7), 591 (14.5), 647 (12).

[*mer*,*cis*-RuCl$_3$(4′MPyP)$_2$(NO)] (4). The product was recrystallized from chloroform–*n*-hexane. R_f = 0.64 (silica gel, $CHCl_3$). Yield: 20 mg (5%). Anal. calcd for $C_{86}H_{58}N_{11}Cl_3O Ru \cdot 2CHCl_3$ (M_W 1707.66): C, 61.9; H, 3.54; N, 9.02; found: C, 61.5; H, 3.70; N, 8.80. ^{1}H-NMR ($CDCl_3$, ppm): 9.61 (m, 4, H2,6), 8.90, 8.83 (m, 16, Hβ), 8.53 (d, 2, H3,5), 8.47 (d, 2, H3,5), 8.19 (m, 4, *o*-H), 8.16 (m, 8, *o*-H), 7.77 (m, 6, *m* + *p*-H), 7.71 (m, 12, *m* + *p*-H), −2.79 (s, 4, NH). Selected IR (KBr, cm^{-1}): 1884 (s, $\nu_{N\equiv O}$). UV-Vis ($CHCl_3$, T = 25 °C) λ_{max}/nm (ε × 10^{-3}/dm^3 mol^{-1} cm^{-1}): 421 (337), 519 (26.7), 555 (17.7), 592 (12.5), 648 (10.5). Crystals suitable for X-ray diffraction were obtained by slow diffusion of *n*-hexane into a chloroform solution of **4**.

[*n*Bu$_4$N]$_4$[(4′TPyP){RuCl$_4$(NO)}$_4$] (5). To a 50 mg amount of 4′TPyP (0.081 mmol) partially dissolved in 35 mL of $CHCl_3$ a 4.5-fold excess of [*n*Bu$_4$N][*trans*-RuCl$_4$(dmso-O)(NO)] (220 mg, 0.37 mmol) was added. The mixture was heated to reflux for 4 h, until no unbound 4′TPyP was observed by TLC (silica gel, $CHCl_3$: EtOH 90 : 10). The product precipitated in the course of the reaction. The suspension was concentrated and the product filtered out and washed with $CHCl_3$. Yield: 270 mg. The raw product was further purified on a chromatographic column; elution with a 95 : 5 mixture $CHCl_3$–EtOH yielded the pure product: 190 mg (85% yield). Anal. calcd for $C_{104}H_{170}N_{16}Cl_{16}O_4Ru_4$ (M_W 2680.09): C, 46.6; H, 6.39; N, 8.36; found: C, 44.3; H, 5.55; N 8.45. ^{1}H-NMR (nitromethane-d_3, ppm): 9.77 (d, H2,6, trans), 9.52 (d, H2,6, cis), 9.20 (v br, Hβ), 8.50 (m, 8, H3,5), 3.25 (m, 32, *n*Bu$_4$N$^+$), 1.72 (m, 32, *n*Bu$_4$N$^+$), 1.40 (m, 32, *n*Bu$_4$N$^+$), 0.96 (t, 48, *n*Bu$_4$N$^+$); (in acetone-d_6): 9.87 (d, H2,6, trans), 9.65 (d, H2,6, cis), 9.17 (v br, Hβ), 8.52 (m, H3,5, cis), 8.48 (m, H3,5, trans), 3.46 (m, 32, *n*Bu$_4$N$^+$), 1.82 (m, 32, *n*Bu$_4$N$^+$), 1.44 (m, 32, *n*Bu$_4$N$^+$), 0.97 (t, 48, *n*Bu$_4$N$^+$). Selected IR (CH_3NO_2, cm^{-1}): 1877, 1867 (s, $\nu_{N\equiv O}$). UV-Vis (CH_3NO_2, T = 25 °C) λ_{max}/nm (relative intensity, %): 422 (100), 515 (11.9), 550 (5.9), 589 (5.9), 645 (3.7). Crystals suitable for X-ray diffraction were obtained by slow diffusion of diethyl ether in a nitromethane solution of **5**.

[*n*Bu$_4$N]$_4$[(Zn · 4′TPyP){RuCl$_4$(NO)}$_4$] (5 · Zn). A 83.5 mg amount of zinc acetate (0.38 mmol) dissolved in 1 mL of methanol was added to 204 mg of **5** (0.076 mmol) dissolved in 10 ml of nitromethane. The reaction proceeded at ambient temperature and its completion was assessed by UV/Vis spectroscopy after 30 min. The reaction mixture was washed with water to remove unreacted zinc acetate and the organic phase was dried over Na_2SO_4, filtered and evaporated to dryness under reduced pressure to yield a reddish solid (205 mg, 98% yield). ^{1}H-NMR (nitromethane-d_3, ppm): 9.72 (d, H2,6, trans), 9.48 (d, H2,6, cis), 9.18 (s, 8, Hβ), 8.45 (m, 8, H3,5), 3.25 (m, 32, *n*Bu$_4$N$^+$), 1.72 (m, 32, *n*Bu$_4$N$^+$), 1.40 (m, 32, *n*Bu$_4$N$^+$), 0.96 (t, 48, *n*Bu$_4$N$^+$). Selected IR (CH_3NO_2, cm^{-1}): 1879, 1867 (s, $\nu_{N\equiv O}$). UV-Vis (CH_3NO_2, T = 25 °C) λ_{max}/nm (relative intensity, %): 429 (100), 558 (7.9), 599 (2.7).

Na$_4$[(4′TPyP){RuCl$_4$(NO)}$_4$] (6). A 119 mg amount of sodium tetraphenylborate (0.34 mmol) dissolved in 2 ml of nitromethane was added to 50 mg of **5** (0.0174 mmol) dissolved in 1 ml of nitromethane. The crude product precipitated from the solution. It was collected on a filter and extensively washed with nitromethane and diethyl ether, and then vacuum dried. Yield: 31 mg (90%). Selected IR (D_2O, cm^{-1}): 1889 (*s*, $\nu_{N\equiv O}$). UV-Vis (H_2O, T = 25 °C) (λ_{max}/nm (relative intensity, %)): 417 (100), 518 (9.3), 550 (5.5), 584 (5.3), 643 (3.4).

Na$_4$[(Zn · 4′TPyP){RuCl$_4$(NO)}$_4$] (6 · Zn). To a 171 mg amount (0.625 mmol) of **5 · Zn** dissolved in 6 mL nitromethane, 428 mg (1.25 mmol) of sodium tetraphenylborate dissolved in 5 ml of nitromethane was added. The crude product precipitated from the solution, was collected on a filter and extensively washed with nitromethane (50 ml) and diethyl ether (10 ml), then vacuum dried. The complex was recrystallized from methanol. Yield: 60 mg (52%). Selected IR (D_2O, cm^{-1}): 1891 (s, $\nu_{N\equiv O}$). By ESI-MS (Fig. 1S, ESI) a relatively broad peak for [Zn · 4′TPyP{RuCl$_4$(NO)}$_4$]$^{4-}$ at m/z = 443–445 was observed. In addition, an MS-MS investigation performed on the 4− parent ion[34] afforded various ions with charges 3−, 2−, and 1−, which all correspond to parts of the compound broken in sensitive places (*i.e.*, [Zn · 4′TPyP{RuCl$_4$(NO)}$_3$]$^{3-}$ at m/z = 499.9, [Zn · 4′TPyP{RuCl$_4$(NO)}$_2$]$^{2-}$ at m/z = 613.3, [Zn · 4′TPyP{RuCl$_4$(NO)}]$^-$ at m/z = 953.2, and [RuCl$_4$(NO)]$^-$ at m/z = 273.9). ^{1}H-NMR (CD_3OD, ppm): 9.73 (d, H2,6, trans), 9.50 (d, H2,6, cis), 9.06 (s, 8, Hβ), 8.40 (m, 8, H3,5). UV-Vis (H_2O, T = 25 °C) λ_{max}/nm (ε × 10^{-3}/dm^3 mol^{-1} cm^{-1}): 429 (160), 568 (16), 607 (7).

X-Ray crystallography¶

Diffraction data of **2** were collected on a Nonius DIP-1030H system equipped with graphite-monochromated Mo-Kα radiation (λ = 0.71073 Å). Intensities of **4** and **5** were measured at the X-ray diffraction beamline of Synchrotron ELETTRA, Trieste (Italy), using a monochromated wavelength of 1.0000 Å. Cell refinement, indexing and scaling of all the data sets were performed using the programs Mosflm and Scala.[35]

The choice of the non-centrosymmetric space group for **5** was confirmed by the successful final cycles of refinement that resolved the disorder of the cations, and furnished a better final R factor. All the structures were solved by direct methods and subsequent Fourier analyses and refined by the full-matrix least-squares method based on F^2 with all observed reflections.[36] Difference Fourier maps revealed the presence of two chloroform molecules in **2** and **4**, and of two nitromethane and a disordered diethyl ether in **5**. All the calculations were performed using the WinGX System, version 1.64.[37]

¶ CCDC reference numbers 265963–265965. See http://www.rsc.org/suppdata/nj/b4/b418855a/ for crystallographic data in .cif or other electronic format.

Crystal data for 2·2(CHCl$_3$). $C_{61}H_{67}Cl_{10}N_7ORu$, M = 1369.79, triclinic, space group $P\bar{1}$, a = 10.833(3), b = 13.688(4), c = 22.584(4) Å, α = 96.46(2)°, β = 96.06(3)°, γ = 106.02(2)°, U = 3165.4(14) Å^3, T = 150 K, Z = 2, D_c = 1.437 g cm^{-3}, μ(Mo-Kα) = 0.716 mm^{-1}, F(000) = 1408, 25 088 reflections measured, 11 615 unique (R_{int} = 0.0831), which were used in all calculations. Final R_1 = 0.0666, wR_2 = 0.1685 for 7410 observed data with $I > 2\sigma(I)$.

Crystal data for 4·2.5(CHCl$_3$)·0.5(C$_6$H$_{14}$). $C_{88}H_{60}Cl_9N_{11}ORu$, M = 1707.59, monoclinic, space group $I\,2/a$, a = 16.978(4), b = 14.283(4), c = 73.283(10) Å, β = 91.28(3)°, U = 17767(7) Å^3, T = 100 K, Z = 8, D_c = 1.354 g cm^{-3}, μ(Mo-Kα) = 1.327 mm^{-1}, F(000) = 7392, 47 057 reflections measured, 9229 unique (R_{int} = 0.1299), which were used in all calculations. Final R_1 = 0.1130, wR_2 = 0.2747 for 5479 observed data with $I > 2\sigma(I)$.

Crystal data for 5·2(CH$_3$NO$_2$)·0.5(OEt$_2$). $C_{108}H_{181}Cl_{16}N_{18}O_{8.50}Ru_4$, M = 2839.19, monoclinic, space group Cc, a = 38.252(6), b = 8.936(3), c = 40.475(6) Å, β = 103.49(3)°, U = 13453(5) Å^3, T = 100 K, Z = 8, D_c = 1.402 g cm^{-3}, μ(Mo-Kα) = 1.951 mm^{-1}, F(000) = 5884, 32 476 reflections measured, 11 985 unique (R_{int} = 0.084), which were used in all calculations. Final R_1 = 0.0549, wR_2 = 0.1522 for 11 713 observed data with $I > 2\sigma(I)$.

Results and discussion

Ru-nitrosyls of 4′MPyP

Treatment of the anionic ruthenium-nitrosyl [nBu$_4$N][*trans*-RuCl$_4$(dmso-O)(NO)] with one equivalent of 4′MPyP (Fig. 1) in refluxing dichloromethane (40 °C, or in chloroform at the same temperature) yielded, according to TLC analysis, a mixture of two main products (besides some unbound porphyrin), **1** and **2**, which have a mobility on silica gel lower than that of 4′MPyP (an indication that the compounds with coordinated 4′MPyP might be charged). Column separation afforded both **1** and **2** in pure form.

The CDCl$_3$ ^{1}H NMR spectrum of **1** (Fig. 2S, ESI) showed only one set of peaks for coordinated 4′MPyP; integration established that there is one molecule of coordinated porphyrin per nBu$_4$N$^+$ cation. Both the NO and Ru–Cl stretching frequencies in **1** were very similar to those found in [nBu$_4$N][*trans*-RuCl$_4$(pyz)(NO)] (pyz = pyrazine),[38] suggesting that **1** has a similar trans geometry: [nBu$_4$N][*trans*-RuCl$_4$(4′MPyP)(NO)] (Scheme 1).

The CDCl$_3$ ^{1}H NMR spectrum of **2** (Fig. 3S, ESI) was very similar to that of **1**, the main difference being the chemical shift of the H2,6 resonance of coordinated 4′MPyP (δ = 9.59 in **2** *vs.* 9.85 in **1**, see Fig. 1 for numbering scheme). In addition, the NO stretching frequency in **2** was *ca.* 20 cm^{-1} lower than in **1** (1851 cm^{-1} in **2** *vs.* 1872 in **1**), suggesting that in **2** NO is trans to a better donor of charge density (or a worse competitor for π back-donation) than in **1**. Indeed, we had previously found for

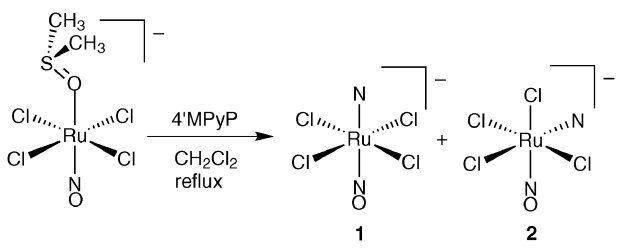

Scheme 1 Reactivity of [nBu$_4$N][*trans*-RuCl$_4$(dmso-O)(NO)] towards 4′MPyP (indicated with N when bound to Ru in **1** and **2**) in refluxing CH_2Cl_2 (40 °C).

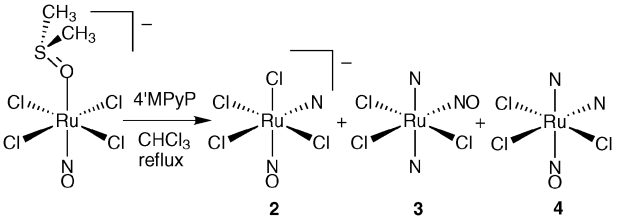

Scheme 2 Reactivity of [nBu$_4$N][*trans*-RuCl$_4$(dmso-O)(NO)] towards 4′MPyP (indicated with N when bound to Ru in **2**, **3**, and **4**) in refluxing $CHCl_3$ (61 °C).

similar ruthenium-nitrosyls that the NO stretching frequency is quite sensitive to the nature of the trans ligand.[31,38] The NO and Ru–Cl stretching frequencies in **2** were very similar to those found in [nBu$_4$N][*cis*-RuCl$_4$(pyz)(NO)],[38] indicating that **2** is the geometrical isomer of **1**: [nBu$_4$N][*cis*-RuCl$_4$(4′MPyP)(NO)]. The geometry of **2** was later confirmed by single crystal X-ray analysis (see below).

When the reaction between 4′MPyP and [nBu$_4$N][*trans*-RuCl$_4$(dmso-O)(NO)] was repeated at higher temperature (61 *vs.* 40 °C), in refluxing chloroform, only traces of compound **1** were found in the NMR spectrum of the raw product, while the resonances of two new Ru-porphyrin adducts, **3** and **4**, were observed besides those of **2** (major product) and of some unbound 4′MPyP (Scheme 2). TLC analysis showed that **3** and **4** have a mobility on silica gel remarkably higher than that of 4′MPyP, an indication that they are neutral species. Column separation of the mixture yielded compounds **3** and **4** in pure form, together with the main reaction product, **2**.

The elemental analysis of both **3** and **4** agreed with the formula [RuCl$_3$(4′MPyP)$_2$(NO)] and, in fact, an increase of the relative amount of **3** and **4**, and a corresponding decrease of **2**, was found upon using a two-fold excess of 4′MPyP in the reaction mixture. The CDCl$_3$ ^{1}H NMR spectrum of **3** (Fig. 2) showed a single set of resonances for coordinated 4′MPyPs and no signals for the nBu$_4$N$^+$ cation. Two geometries, either [*mer*,*trans*-RuCl$_3$(4′MPyP)$_2$(NO)] or [*fac*-RuCl$_3$(4′MPyP)$_2$(NO)], are compatible with the NMR spectrum of **3**. In both isomers the nitrosyl is trans to a Cl, so that the NO stretching frequency is not diagnostic for distinguishing between them. The CDCl$_3$ ^{1}H NMR spectrum of **4** (Fig. 2) was characterized by two partially resolved sets of resonances for two inequivalent 4′MPyP ligands; in particular, the H3,5 resonances for the two coordinated porphyrins were well-resolved. In addition, the phenyl proton resonances (*i.e.*, *o*H and *m* + *p*H) were split

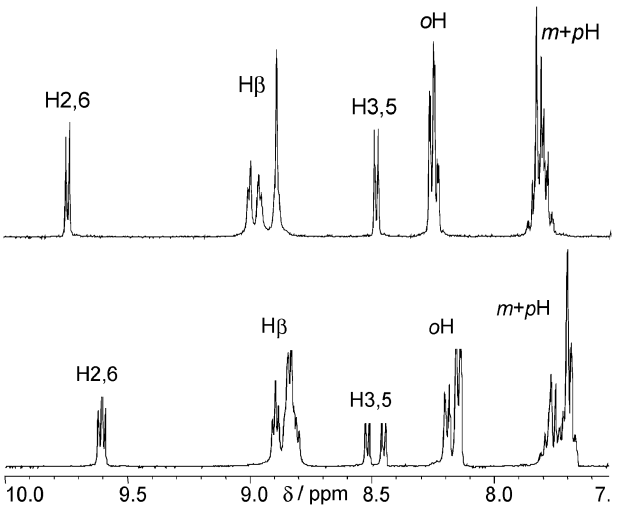

Fig. 2 ^{1}H NMR spectrum (CDCl$_3$, aromatic region) of [*mer*,*trans*-RuCl$_3$(4′MPyP)$_2$(NO)] (**3**) (top) and [*mer*,*cis*-RuCl$_3$(4′MPyP)$_2$(NO)] (**4**) (bottom).

into two sets of multiplets in a 1 : 2 ratio; as we have established,[24] this is the typical signature for two mutually cis-coordinated pyridylporphyrins in free rotation about the metal–pyridyl axis. The signals of the major set, shifted upfield by about 0.04 ppm compared to those of the minor set, were assigned to the two phenyl rings cis to the pyridyl ring coordinated to Ru (positions 10 and 20, see Fig. 1). Such an upfield shift is caused by the rotation of each porphyrin about the Ru–pyridyl axis, which brings the phenyl rings at the 10 and 20 positions into the shielding cone of the adjacent porphyrin. Thus, the NMR data indicated the [*mer*,*cis*-$RuCl_3(4'MPyP)_2(NO)$] geometry for **4**, which was confirmed by X-ray structural analysis (see below). Since this NMR signature is absent in the spectrum of its geometrical isomer, we attribute to **3** a [*mer*,*trans*-$RuCl_3(4'MPyP)_2(NO)$] geometry (rather than a [*fac*-$RuCl_3(4'MPyP)_2(NO)$] geometry that would imply two cis-coordinated porphyrins).

The solid state NO stretching frequency in **3** (1861 cm^{-1}) is *ca.* 25 cm^{-1} lower than in **4**, as expected for an NO trans to Cl (in both possible isomers of **3**) compared to an NO trans to a pyridyl-N (see **1** and **2** above). The higher NO stretching frequencies of **3** and **4** compared to **1** and **2** are attributed to the different charge, as in neutral complexes (**3** and **4**) the back-donation to NO is expected to be lower than in anionic species (**1** and **2**).

Ru-nitrosyls of 4′TPyP

Treatment of 4′TPyP with a four-fold excess of [$n$$Bu_4N$][*trans*-$RuCl_4$(dmso-O)(NO)] in refluxing chloroform yielded a product (**5**) in which, according to NMR spectroscopy, all four pyridyl rings of the porphyrin are coordinated to $[RuCl_4(NO)]^-$ fragments. Integration established that there are four nBu_4N^+ cations per porphyrin, suggesting for **5** the following stoichiometry: [$n$$Bu_4N$]$_4$[4′TPyP{$RuCl_4(NO)$}$_4$]. The CD_3NO_2 ^{1}H NMR spectrum of **5** (Fig. 4S, ESI) was characterized by two well-resolved doublets for 2,6 protons at δ = 9.77 and 9.52, respectively, in a *ca.* 1 : 2.5 intensity ratio; comparison with the H2,6 resonances of **1** and **2** suggested that they might belong to pyridyl rings coordinated to *trans*- and *cis*-$[RuCl_4(NO)]^-$ fragments, respectively. The corresponding resonances for the 3,5 protons partially overlap at *ca.* δ = 8.5 (they are resolved in acetone-d_6). It is reasonable to assume that the H2,6 and H3,5 resonances of each pyridyl ring in **5** are influenced only by the geometry of the metal fragment connected to that ring, and not by the geometry of the other Ru fragments bound to the porphyrin. The solid state IR spectrum of **5** (KBr) had a single, relatively broad NO stretching band centered at 1870 cm^{-1}; in CH_3NO_2 solution this band showed two partially resolved maxima at 1877 and 1867 cm^{-1} that, by comparison with the spectra of **1** and **2**, might be attributed to the *trans*- and *cis*-$[RuCl_4(NO)]^-$ fragments, respectively.

The CD_3NO_2 ^{1}H NMR spectrum of **5** deserves some further comments. At 25 °C the βH resonance was very broad and sharpened upon raising the temperature;‖ a sharp singlet that integrated as the sum of the two H2,6 resonances (*i.e.*, 8H) was observed at T = 80 °C (the pyridyl resonances were substantially unaffected by changes in temperature). For T < 0 °C, the βH resonance splits into two equally intense and relatively broad signals that are connected by an exchange cross-peak in the NOESY spectrum, but show no connection in the H–H COSY spectrum. Finally, the NH resonance had a very low intensity in each solvent tested and over the whole range of temperatures examined. The temperature dependence of the NMR spectrum of **5** suggests the existence of a dynamic process with an intermediate rate on the NMR time scale at room temperature that involves mainly the porphyrin βH and NH protons and not the pyridyl protons. A geometrical isomerization between the *cis*- and *trans*-$[RuCl_4(NO)]^-$ fragments seems unlikely, as it was not observed in compounds **1–4** and the NMR spectrum of **5** remained unchanged for weeks. Restricted rotation of the ruthenated pyridyl rings would be expected to influence also the pyridyl resonances, and was not observed for compounds **1–4**. As the zincated adduct **5 · Zn** has a normal NMR spectrum (Fig. 3), it seems likely that the unusual pyrrole and NH resonances of **5** are due to protonation equilibria involving the inner N atoms,** rather than to aggregation phenomena that would be expected to affect all resonances.[39,40] Anionic tetraphenylporphyrins are normally expected to have higher pK_a values because of the inductive effects of the anionic substituents.[40]

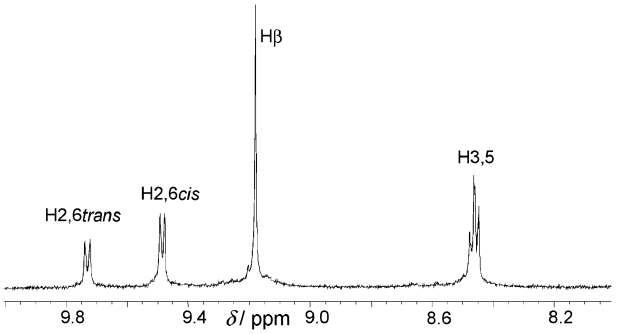

Fig. 3 ^{1}H NMR spectrum (CD_3NO_2, 4′TPyP region) of [$n$$Bu_4N$]$_4$[Zn · 4′TPyP{$RuCl_4(NO)$}$_4$] (**5 · Zn**).

The X-ray molecular structure of **5** (see below) showed the presence of two isomers differing in the geometry of the $[RuCl_4(NO)]^-$ fragments: *ca.* 60% of [(4′TPyP){*cis*-$RuCl_4(NO)$}$_2${*trans*-$RuCl_4(NO)$}$_2$]$^{4-}$ (**5a**) and *ca.* 40% of [(4′TPyP){*cis*-$RuCl_4(NO)$}$_3${*trans*-$RuCl_4(NO)$}]$^{4-}$ (**5b**) (Fig. 4). In **5a** the fragments of equal geometry are coordinated to pyridyl rings in mutually trans positions. According to the solid state analysis, the overall ratio between the *trans*- and *cis*-$[RuCl_4(NO)]^-$ fragments is *ca.* 1 : 1.5, while in solution it is *ca.* 1 : 2.5. Thus, it seems likely that the composition in solution, in terms of isomers, is different from that found in the crystals.

Treatment of **5** with zinc acetate yielded the corresponding [$n$$Bu_4N$]$_4$[Zn · 4′TPyP{$RuCl_4(NO)$}$_4$] (**5 · Zn**) almost quantitatively. The room temperature ^{1}H NMR spectrum of **5 · Zn** in CD_3NO_2 or acetone-d_6 is similar to that of **5** but simpler, as the βH resonance is a sharp singlet (Fig. 3).

The UV-Vis spectra of compounds **1–5** are completely dominated by the porphyrin(s) absorption bands. The weak and broad bands of the $[RuCl_4(NO)]^{-1}$ or $RuCl_3(NO)$ fragments, which are normally found at *ca.* 480 nm, are masked by the porphyrin Q bands.

Description of the X-ray structures

The molecular structures of **2** (anion only) and **4** are shown in Figs. 5 and 6, respectively; a selection of bond lengths, angles and other geometrical parameters is reported in Table 1. The dihedral angle between the two porphyrins in **4** is 83.78(9)°.

The linear nitrosyl moiety is cis to the coordinated 4′MPyP in **2**, while in **4** it is trans to one 4′MPyP (and cis to the other). In both compounds the Ru centers display a slightly distorted

‖ The ^{1}H NMR spectra of **1** and **2** indicate that, as might be expected, the pyrrole resonances are not very sensitive to the geometry of the peripheral $[RuCl_4(NO)]^-$ fragments. In any case, a complex set of overlapping multiplets, rather than a broad, temperature-dependent signal, would be expected for βH in **5**.

** Protonation equilibria of the type $H_2Por^{4-} + H^+ \rightleftharpoons H_3Por^{3-}$ and $H_3Por^{3-} + H^+ \rightleftharpoons H_4Por^{2-}$ have been proposed to occur in aqueous solution for porphyrins similar to **5**, featuring four negatively charged substituents in peripheral positions (see ref. 40). Titration experiments with **5** were prevented by its lack of solubility in water.

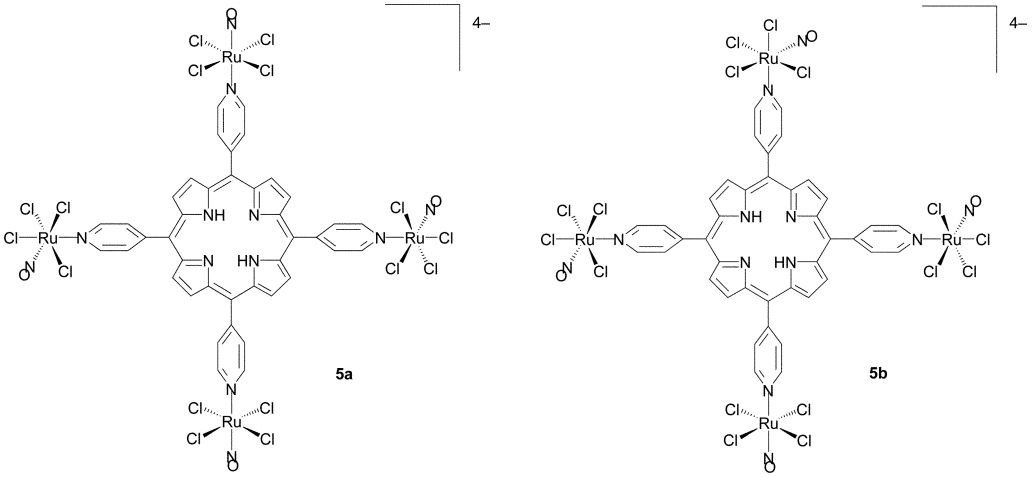

Fig. 4 Schematic drawings of $[(4'TPyP)\{cis\text{-}RuCl_4(NO)\}_2\{trans\text{-}RuCl_4(NO)\}_2]^{4-}$ (**5a**) and $[(4'TPyP)\{cis\text{-}RuCl_4(NO)\}_3\{trans\text{-}RuCl_4(NO)\}]^{4-}$ (**5b**).

octahedral geometry with comparable values of coordination bond lengths and angles. However, there is a fair indication that Ru–NO and N–O bond lengths are slightly longer and shorter, respectively, compared to those already reported for analogous Ru nitrosyls containing py and dmso ligands.[31,38]

Most of the *meso* pyridyl and phenyl rings in **2** and **4** are oriented approximately perpendicular to the porphyrin mean plane (Table 1), even though in some cases dihedral angles as low as 54.8° (phenyl ring *b* in **2**, Fig. 5), and 47.7° (phenyl ring *f* in **4**, Fig. 6) were found. The latter is likely induced by crystal packing effects since the ring is stacking with porphyrin units of adjacent molecules.

The coordinated porphyrins exhibit considerable distortions from planarity. In **2** the best-fit plane through 4′MPyP atoms shows utmost displacements of ±0.24(1) Å, with the Ru atom at 0.104(5) Å from it. In **4** the atom deviations are remarkably larger, being ±0.11(1) Å in the chromophore cis to NO and ±0.43(1) Å in the other, with the metal displaced by 0.50(1) and 1.65(1) Å from each 4′MPyP mean plane, respectively. The latter value is induced by a significant bending of the porphyrin moiety (Fig. 5S, ESI).

The crystal structure analysis of **5** indicates a tetranuclear anion composed by the 4′TPyP macrocycle bound to four $[RuCl_4(NO)]^-$ units (Fig. 7). Coordination bond lengths and geometrical parameters are reported in Table 2. The pseudo-centrosymmetric arrangement of the molecule shows two NO groups symmetrically located in cis and two in trans positions with respect to the *meso* pyridyl rings of the porphyrin. However, the nitrosyl ligand was found to be disordered in the coordination sphere of Ru(3). A satisfactory refinement of occupancies was obtained only with the ligand trans to the pyridyl ring, providing a NO : Cl ratio of 0.59 : 0.41, with the residual nitrosyl spread over the (other) cis located chlorides.

All the Ru atoms in **5** display the expected octahedral geometry with an almost linear coordination for the nitrosyl ligands with the exception of the disordered one, which evidences a small bent [O(3)–N(3)–Ru(3) = 159(3)°]. The Ru–NO [1.764(8)–1.834(15) Å] and Ru–N(py) [2.107(8)–2.140(8) Å] bond lengths, are all comparable within 3σ, but the low accuracy on the NO values does not allow a detailed comment. The Ru–Cl distances vary in a large range from 2.341(4) to 2.388(3) Å, with shorter values for those trans to nitrosyl groups. The atoms of the porphyrin ring in **5** are coplanar within ±0.107(8) Å, with the peripheral Ru ions remarkably displaced from it [−0.849(6), 0.745(7), 1.196(7), and −0.614(7) Å for Ru(1) to Ru(4), respectively], and with the pyridyl rings arranged almost normal to the mean plane. These distortions are evident from the side view of the complex, reported in Fig. 8.

The nitromethane and diethyl ether solvent molecules, which are distributed in the crystal among the tetranuclear complexes and the nBu_4N^+ cations, did not evidence any unusual short contacts.

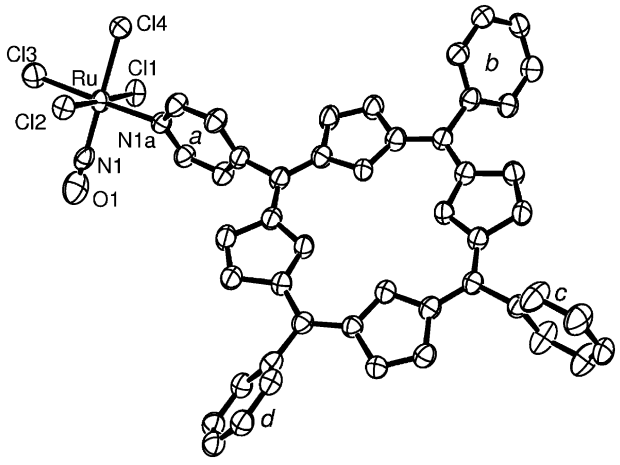

Fig. 5 Molecular structure of the complex anion of $[nBu_4N][cis\text{-}RuCl_4(4'MPyP)(NO)]$ (**2**; ORTEP[41] drawing, thermal ellipsoids at 40% probability).

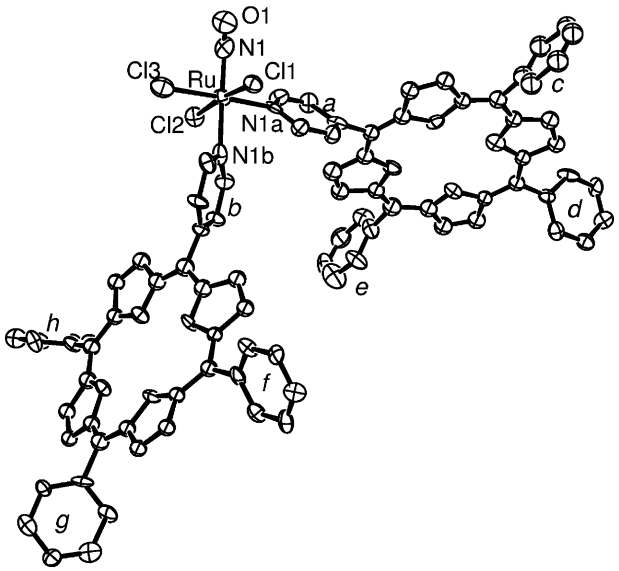

Fig. 6 Molecular structure of complex $[mer,cis\text{-}RuCl_3(4'MPyP)_2(NO)]$ (**4**; ORTEP[41] drawing, thermal ellipsoids at 40% probability).

Table 1 Selected bond lengths (Å), angles (°) and dihedral angles (°) between porphyrin and pyridyl or phenyl planes in complexes **2** and **4**

	2	**4**
Ru–N(1)	1.843(6)	1.760(15)
Ru–N(1a)	2.127(4)	2.120(12)
Ru–N(1b)	—	2.133(13)
Ru–Cl(1)	2.385(2)	2.374(4)
Ru–Cl(2)	2.377(2)	2.356(4)
Ru–Cl(3)	2.336(2)	2.358(5)
Ru–Cl(4)	2.345(2)	—
O(1)–N(1)–Ru	173.1(7)	167.7(19)
Porph–py[a]	79.1(1) *a*	68.8(4) *a*, 58.3(3) *b*
Porph–ph[a]	54.8(1) *b*	67.6(5) *c*, 62.8(4) *d*
	89.6(2) *c*	72.5(5) *e*, 47.7(3) *f*
	88.3(2) *d*	50.6(4) *g*, 64.0(3) *h*

[a] Rings labelled in Figs. 5 and 6.

Table 2 Selected bond lengths (Å), angles (°) and dihedral angles (°) between porphyrin and pyridyl planes in the complex anion of **5**

Ru(1)–N(1)	1.802(9)	Ru(3)–N(3)[a]	1.834(15)
Ru(1)–N(1a)	2.136(10)	Ru(3)–N(1c)	2.140(10)
Ru(1)–Cl(10)	2.341(4)	Ru(3)–Cl(30)	2.373(5)
Ru(1)–Cl(11)	2.381(3)	Ru(3)–Cl(31)	2.375(4)
Ru(1)–Cl(12)	2.378(4)	Ru(3)–Cl(32)	2.360(4)
Ru(1)–Cl(13)	2.372(3)	Ru(3)–Cl(33)	2.343(4)
O(1)–N(1)–Ru(1)	171.7(11)	O(3)–N(3)–Ru(3)	159(3)
Ru(2)–N(2)	1.816(9)	Ru(4)–N(4)	1.764(8)
Ru(2)–N(1b)	2.140(8)	Ru(4)–N(1d)	2.107(8)
Ru(2)–Cl(20)	2.384(3)	Ru(4)–Cl(40)	2.388(3)
Ru(2)–Cl(21)	2.350(3)	Ru(4)–Cl(41)	2.347(3)
Ru(2)–Cl(22)	2.367(3)	Ru(4)–Cl(42)	2.368(3)
Ru(2)–Cl(23)	2.365(4)	Ru(4)–Cl(43)	2.371(4)
O(2)–N(2)–Ru(2)	172.9(11)	O(4)–N(4)–Ru(4)	169.8(9)
Porph–py[b]	74.2(2) *a*, 82.9(2) *b*, 79.1(3) *c*, 68.7(2) *d*		

[a] The nitrosyl group disordered over a Cl. [b] Ring labels indicated in Fig. 7.

A water-soluble porphyrin: $Na_4[Zn \cdot 4'TPyP\{RuCl_4(NO)\}_4]$

Treatment of **5** with sodium tetraphenylborate in nitromethane solution afforded the corresponding sodium derivative $Na_4[4'TPyP\{RuCl_4(NO)\}_4]$ (**6**) in reasonable yield. Compound **6** is well-soluble in water; however, at millimolar concentrations, formation of a fluffy purple precipitate became apparent within hours after dissolution and became almost quantitative after 1 day, as judged by the residual colour of the solution. The precipitate did not re-dissolve even upon warming of the mixture. Spectroscopic investigations could be performed only on fresh solutions. The D_2O ^1H NMR spectrum of **6** showed very broad resonances exclusively. However, the UV-Vis spectrum of **6** in water revealed the typical absorption maxima of a free-base porphyrin (Soret band at 415 nm, and Q bands at 515, 550, 579, 640 nm) and the solution IR spectrum (D_2O) showed the strong N–O stretching absorption at 1889 cm^{-1}.

On the contrary, the corresponding compound with the zincated porphyrin, $Na_4[Zn \cdot 4'TPyP\{RuCl_4(NO)\}_4]$ (**6 · Zn**), obtained from **5 · Zn** by a similar procedure, afforded stable solutions both in water and in methanol. In aqueous solution the NO stretching of **6 · Zn** occurred at 1891 cm^{-1}. The nature of **6 · Zn** was confirmed by ESI-MS spectrometry. Its ^1H NMR spectrum showed exclusively very broad peaks in D_2O, also at 70 °C, while it gave well-resolved and relatively sharp resonances in CD_3OD, even at room temperature (Fig. 6S, ESI), suggesting that aggregation occurs in aqueous solution but much less in methanol. Since in porphyrin chemistry the detection of aggregation is normally performed through UV/Vis spectroscopy, we measured the absorption spectra of **6 · Zn** in water and methanol to verify any spectral modification. Despite the NMR results in D_2O, we did not observe any deviation from Beer's law in the range 10^{-4}–10^{-7} M in either solvent. However, even though the frequencies of the absorption maxima of **6 · Zn** in water and methanol are practically the same, the Soret B-band in water is significantly broader than in methanol ($\Delta_{1/2}$ 38 nm in H_2O *vs.* 23 nm in MeOH, concentration 1×10^{-6} M), which has been related to the formation of porphyrin stacks without defined geometry.[42]

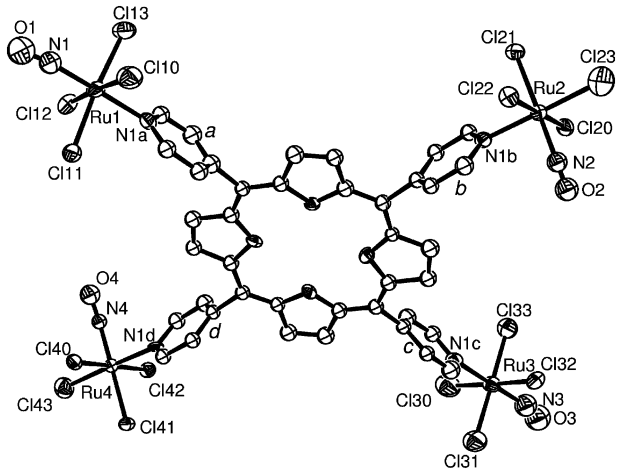

Fig. 7 View of the anion of the tetranuclear complex $[nBu_4N]_4[4'TPyP\{RuCl_4(NO)\}_4]$ (**5**) with the essential atom labelling scheme (ORTEP[41] drawing, thermal ellipsoids at 50% probability). Of the disordered NO/Cl ligands at Ru(3) only the nitrosyl (at higher occupancy, 59%) is shown.

Fig. 8 Side view of the complex anion of $[nBu_4N]_4[4'TPyP\{RuCl_4(NO)\}_4]$ (**5**) viewed along the Ru(2)–Ru(4) direction.

Conclusions

With the aim of making water-soluble *meso*-4′pyridylporphyrins peripherally decorated with Ru-nitrosyls, we investigated first the reactivity of $[nBu_4N][trans\text{-}RuCl_4(dmso\text{-}O)(NO)]$ towards 4′MPyP. The nature of the products depended on the reaction conditions. When the reaction was performed in refluxing dichloromethane a mixture of the two mono-substituted geometrical isomers, $[nBu_4N][trans\text{-}RuCl_4(4'MPyP)(NO)]$ (**1**) and $[nBu_4N][cis\text{-}RuCl_4(4'MPyP)(NO)]$ (**2**), was selectively obtained. Conversely, the di-substituted compounds, $[mer,trans\text{-}RuCl_3(4'MPyP)_2(NO)]$ (**3**) and $[mer,cis\text{-}RuCl_3(4'MPyP)_2(NO)]$ (**4**), were obtained, together with the mono-substituted complex **2**, when the reaction was performed at higher temperature (refluxing chloroform). All compounds **1–4** were obtained in pure form by column chromatography and thoroughly characterized by IR and NMR spectroscopy. The molecular structures of **2** and **4** were determined by X-ray crystallography (Figs. 5 and 6).

Thus, the explorative investigation with 4′MPyP indicated the best conditions for performing the reaction between 4′TPyP and a four-fold excess of the ruthenium precursor, which led to the isolation of $[nBu_4N]_4[4'TPyP\{RuCl_4(NO)\}_4]$ (**5**). ^1H NMR spectroscopy evidenced that in solution *ca.* 30% of the peripheral ruthenium-nitrosyl fragments bound to the pyridyl rings have a $trans\text{-}[RuCl_4(NO)]^-$ geometry, while the remaining 70% have a $cis\text{-}[RuCl_4(NO)]^-$ geometry. In the solid

state the X-ray structure (Fig. 7) evidenced the presence of two isomers: *ca.* 60% of $[(4'TPyP)\{cis\text{-}RuCl_4(NO)\}_2\{trans\text{-}RuCl_4(NO)\}_2]^{4-}$ (**5a**) and *ca.* 40% of $[(4'TPyP)\{cis\text{-}RuCl_4(NO)\}_3\{trans\text{-}RuCl_4(NO)\}]^{4-}$ (**5b**). In **5a** the fragments of equal geometry are coordinated to pyridyl rings in mutually trans positions. Insertion of zinc afforded $[nBu_4N]_4[Zn\cdot 4'TPyP\{RuCl_4(NO)\}_4]$ (**5·Zn**) almost quantitatively.

Treatment of **5·Zn** with sodium tetraphenylborate in nitromethane solution afforded the corresponding sodium derivative $Na_4[Zn\cdot 4'TPyP\{RuCl_4(NO)\}_4]$ (**6·Zn**) in good yield. Compound **6·Zn** gives stable solutions both in water and in methanol, while the corresponding free-base derivative $Na_4[4'TPyP\{RuCl_4(NO)\}_4]$ (**6**) gives rise to a fluffy purple precipitate (probably due to strong aggregation) soon after dissolution in water. Electronic absorption and ^1H NMR spectroscopies showed that **6·Zn** aggregates is aqueous solution, also at relatively high temperature (70 °C) and low concentration (10^{-7} M), but much less so in methanol.

In conclusion, $[nBu_4N][trans\text{-}RuCl_4(dmso\text{-}O)(NO)]$ proved to be a suitable precursor for appending negatively charged $[RuCl_4(NO)]^-$ fragments to the peripheral N atoms of *meso*-4′pyridylporphyrins. Exchange of nBu_4N^+ for Na^+ eventually led to the new, water-soluble tetraruthenated porphyrin $Na_4[Zn\cdot 4'TPyP\{RuCl_4(NO)\}_4]$, whose anti-viral properties are currently being investigated.

Acknowledgements

Acknowledgements are made for financial support to the donors of The Petroleum Research Fund, administered by the ACS, (grant ACS PRF# 38892-AC3) and to MIUR (PRIN no. 2003035553). We wish to thank Engelhard Italiana S.p.A. for a generous loan of hydrated $RuCl_3$. We are grateful to Dr Isam Khalaila and Prof. Paul Dyson (Ecole Polytechnique Federale de Lausanne, EPLF-BCH, Lausanne, Switzerland) for performing the ESI-MS spectra and for helpful discussion. The CNR staff at ELETTRA (Trieste) are acknowledged for help in the use of the facility supported by CNR and by Elettra Scientific Division.

References

1 P. D. Harvey, in *The Porphyrin Handbook*, eds. K. M. Kadish, K. M. Smith and R. Guilard, Academic Press, Boston, 2003, vol. 18, pp. 63–249.

2 (*a*) R. Lauceri, R. Purello, S. J. Shetty and M. G. H. Vicente, *J. Am. Chem. Soc.*, 2001, **123**, 5835; (*b*) D. H. Tjahjono, S. Mima, T. Akutsu, N. Yoshioka and H. Inoue, *J. Inorg. Biochem.*, 2001, **85**, 219; (*c*) R. F. Pasternack and E. J. Gibbs, in *Metal Ions in Biological Systems*, eds. A. Siegel and H. Siegel, Marcel Dekker, New York, 1996, vol. 33, pp. 367–397; (*d*) L. A. Lipscomb, F. X. Zhou, S. R. Presnell, R. J. Woo, M. E. Peck, R. R. Plaskon and L. D. Williams, *Biochemistry*, 1996, **35**, 2818; (*e*) N. E. Mukundan, G. Pethö, D. W. Dixon and L. G. Marzilli, *Inorg. Chem.*, 1995, **34**, 3677; (*f*) U. Sehlstedt, S. K. Kim, P. Carter, J. Goodisman, J. F. Vollano, B. Nordén and J. C. Dabrowiak, *Biochemistry*, 1994, **33**, 417; (*g*) L. G. Marzilli, G. Pethö, M. Lin, M. S. Kim and D. W. Dixon, *J. Am. Chem. Soc.*, 1992, **114**, 7575; (*h*) R. J. Fiel, *J. Biomol. Struct. Dyn.*, 1989, **6**, 1259; (*i*) R. F. Pasternak and E. J. Gibbs, in *Metal DNA Chemistry*, ed. T. Tullius, American Chemical Society, Washington, DC, 1989, pp. 59–73; (*j*) G. Dougherty, *J. Inorg. Biochem.*, 1988, **34**, 95.

3 (*a*) L. H. Hurley, R. T. Wheelhouse, D. Sun, S. M. Kerwin, M. Salazar, O. Y. Fedoroff, F. X. Han, H. Han, E. Izbicka and D. D. Von Hoff, *Pharmacol. Therapeut.*, 2000, **85**, 141; (*b*) F. X. Han, R. T. Wheelhouse and L. H. Hurley, *J. Am. Chem. Soc.*, 1999, **121**, 3561; (*c*) I. Haq, J. O. Trent, B. Z. Chowdhry and T. C. Jenkins, *J. Am. Chem. Soc.*, 1999, **121**, 1768.

4 For a review on the medical aspects of DNA-porphyrin interactions see: L. G. Marzilli, *New J. Chem.*, 1990, **14**, 409.

5 (*a*) B. Meunier, A. Robert, G. Pratviel and J. Bernadou, in *The Porphyrin Handbook*, eds. K. M. Kadish, K. M. Smith and R. Guilard, Academic Press, Boston, 2000, vol. 4, pp. 119–188; (*b*) S. Mettath, B. R. Munson and R. K. Pandey, *Bioconjugate Chem.*, 1999, **10**, 94; (*c*) B. Harmitage, *Chem. Rev.*, 1998, **98**, 1171; (*d*) M. Hartmann, A. Robert, V. Duarte, B. K. Keppler and B. Meunier, *J. Biol. Inorg. Chem.*, 1997, **2**, 427; (*e*) G. Pratviel, J. Bernadou and B. Meunier, in *Metal Ions in Biological Systems*, eds. A. Siegel and H. Siegel, Marcel Dekker, New York, 1996, vol. 33, pp. 399–426.

6 (*a*) D. H. Hilmey, M. Abe, M. I. Nelen, C. E. Stilts, G. A. Baker, S. N. Baker, F. V. Bright, S. R. Davies, S. O. Gollnick, A. R. Oseroff, S. L. Gibson, R. Hilf and M. R. Detty, *J. Med. Chem.*, 2002, **45**, 449; (*b*) R. K. Pandey and G. Zheng, in *The Porphyrin Handbook*, eds. K. M. Kadish, K. M. Smith and R. Guilard, Academic Press, Boston, 2000, vol. 6, pp. 157–230;; (*c*) H. Ali and J. E. van Lier, *Chem. Rev.*, 1999, **99**, 2379; (*d*) T. J. Dougherty, C. J. Gomer, B. W. Henderson, G. Jori, D. Kessel, M. Korbelik, J. Moan and Q. Peng, *J. Natl. Cancer Inst.*, 1998, **90**, 889; (*e*) E. Sternberg and D. Doplhin, *Tetrahedron*, 1998, **54**, 4151; (*f*) R. W. Boyle and D. Dolphin, *Photochem. Photobiol.*, 1996, **64**, 469; (*g*) B. W. Henderson and T. J. Dougherty, *Photochem. Photobiol.*, 1992, **55**, 145.

7 (*a*) R. J. Fiel, E. Mark, T. Button, S. Gilani and D. Musser, *Cancer Lett.*, 1988, **40**, 23; (*b*) D. Kessel, P. Thompson, K. Saatio and K. D. Nantwi, *Photochem. Photobiol.*, 1987, **45**, 787.

8 (*a*) A. R. M. Chen-Collins, D. W. Dixon, A. N. Vzorov, L. G. Marzilli and R. W. Compans, *BMC Infect. Dis.*, 2003, **3**, 9, and references therein; (*b*) A. N. Vzorov, D. W. Dixon, J. S. Trommel, L. G. Marzilli and R. W. Compans, *Antiviral Res.*, 2003, **59**, 99; (*c*) R. Song, M. Witvrouw, D. Schols, A. Robert, J. Balzarini, E. De Clercq, J. Bernadou and B. Meunier, *Antiviral Chem. Chemother.*, 1997, **8**, 85; (*d*) D. W. Dixon, M. S. Kim, V. Kumar, G. Obara, L. G. Marzilli and R. F. Schinazi, *Antiviral Chem. Chemother.*, 1992, **3**, 279; (*e*) D. W. Dixon, R. Schinazi and L. G. Marzilli, *Ann. N.Y. Acad. Sci.*, 1990, **616**, 511.

9 (*a*) L. Ding, G. Etemad-Moghadam, S. Cros, C. Auclair and B. Meunier, *J. Med. Chem.*, 1991, **34**, 900; (*b*) L. Ding, G. Etemad-Moghadam and B. Meunier, *Biochemistry*, 1990, **29**, 7868; (*c*) L. Ding, C. Casas, G. Etemad-Moghadam and B. Meunier, *New J. Chem.*, 1990, **14**, 421.

10 (*a*) M. G. H. Vicente, D. J. Nurco, S. J. Shetty, C. J. Medforth and K. M. Smith, *Chem. Commun.*, 2001, 483; (*b*) M. G. H. Vicente, S. J. Shetty, A. Wickramasinghe and K. M. Smith, *Tetrahedron Lett.*, 2000, **41**, 7623; (*c*) S. B. Kahl, D. D. Joel, M. M. Nawrocky, P. L. Micca, K. P. Tran, G. C. Finkel and D. N. Slatkin, *Proc. Natl. Acad. Sci. USA*, 1990, **87**, 7265.

11 (*a*) B. J. White and H. J. Harmon, *Biosens. Bioelectron.*, 2002, **17**, 463; (*b*) S. C. Moon, J.-H. Shin, B. H. Jeong, H. S. Kim, B. S. Yu, J.-S. Lee, B. S. Lee and S. K. Namgoong, *Bioorg. Med. Chem. Lett.*, 2000, **10**, 1435; (*c*) B. H. Lee, M. B. Park and B. S. Yu, *Bioorg. Med. Chem. Lett.*, 1998, **8**, 1467.

12 Y. Watanabe, in *The Porphyrin Handbook*, eds. K. M. Kadish, K. M. Smith and R.Guilard, Academic Press, Boston, 2000, **vol. 4**, pp. 97–117.

13 (*a*) F. Hindre, M. Le Plouzennec, J. D. de Certaines, M. T. Foultier, T. Patrice and G. Simonneaux, *J. Magn. Reson. Imaging*, 1993, **3**, 59; (*b*) M. Hoehn-Berlage, D. Norris, K. Bockhorst, R.-I. Ernestus, O. Kloiber, P. Bonnekoh, D. Leibfritz and K.-A. Hossman, *Magn. Reson. Med.*, 1992, **27**, 201; (*c*) D. A. Place, P. J. Faustino, K. K. Berghmans, P. C. M. van Zijl, A. S. Chesnick and J. S. Cohen, *Magn. Reson. Imaging*, 1992, **10**, 919; (*d*) R. J. Fiel, D. A. Musser, E. H. Mark, R. Mazurchuk and J. J. Alletto, *Magn. Reson. Imaging*, 1990, **8**, 255; (*e*) N. J. Patronas, J. S. Cohen, R. H. Knop, A. J. Dwyer, D. Colcher, J. Lundy, F. Mornex, P. Hambright, M. Sohn and C. E. Myers, *Cancer Treat. Rep.*, 1986, **70**, 391.

14 D. Dolphin, *Can. J. Chem.*, 1994, **72**, 1005.

15 (*a*) M. Subbarayan, S. J. Shetty, T. S. Srivastava, O. P. D. Noronha, A. M. Samuel and H. Mukhtar, *Biochem. Biophys. Res. Commun.*, 2001, **281**, 32; (*b*) G. D. Zanelli and A. C. Kaelin, *Br. J. Radiol.*, 1981, **54**, 403; (*c*) P. Hambright, R. Fawwaz, P. Valk, J. McRae and A. J. Bearden, *Bioinorg. Chem.*, 1975, **5**, 87.

16 (*a*) J. Bernadou, M. Bonnafous, G. Labat, P. Loiseau and B. Meunier, *Drug Metab. Dispos.*, 1991, **19**, 360; (*b*) G. Gasmi, M. Pasdeloup, G. Pratviel, M. Pitie, J. Bernadou and B. Meunier, *Nucleic Acid Res.*, 1991, **19**, 2835.

17 (*a*) B. R. James, G. G. Meng, J. J. Posakony, J. A. Ravensbergen, C. J. Ware and K. A. Skov, *Metal-Based Drugs*, 1996, **3**, 85; (*b*) G. G. Meng, B. R. James and K. A. Skov, *Can. J. Chem.*, 1994, **72**, 1894; (*c*) G. G. Meng, B. R. James, K. A. Skov and M. Korbelik, *Can. J. Chem.*, 1994, **72**, 2447.

18 M. Sirish, V. A. Chertkov and H.-J. Schneider, *Chem.-Eur. J.*, 2002, **8**, 1181.

19 R.-H. Jin, S. Aoki and K. Shima, *Chem. Commun*., 1996, 1939.
20 (*a*) C. Lottner, K.-C. Bart, G. Bernhardt and H. Brunner, *J. Med. Chem*., 2002, **45**, 2079; (*b*) C. Lottner, K.-C. Bart, G. Bernhardt and H. Brunner, *J. Med. Chem*., 2002, **45**, 2064; (*c*) H. Brunner, K.-M. Schellerer and B. Treittinger, *Inorg. Chim. Acta*, 1997, **264**, 67; (*d*) H. Brunner and H. Obermeier, *Angew. Chem., Int. Ed. Engl*., 1994, **33**, 2214.
21 (*a*) R. Song, Y.-S. Kim, C. O. Lee and Y. S. Sohn, *Tetrahedron Lett*., 2003, **44**, 1537; (*b*) R. Song, Y.-S. Kim and Y. S. Sohn, *J. Inorg. Biochem*., 2002, **83**, 83.
22 F. C. Anson, C. Shi and B. Steiger, *Acc. Chem. Res*., 1997, **30**, 437.
23 H. E. Toma and K. Araki, *Coord. Chem. Rev*., 2000, **196**, 307, and references therein.
24 E. Alessio, M. Macchi, S. L. Heath and L. G. Marzilli, *Inorg. Chem*., 1997, **36**, 5614.
25 H. Winnischofer, F. M. Engelmann, H. E. Toma, K. Araki and H. R. Rechenberg, *Inorg. Chim. Acta*, 2002, **338**, 27.
26 (*a*) M. Castriciano, A. Romeo, R. Romeo and L. Monsù Scolaro, *Eur. J. Inorg. Chem*., 2002, 531; (*b*) M. C. Lensen, M. Castriciano, R. G. E. Coumans, J. Foekema, A. E. Rowan, L. Monsù Scolaro and R. J. M. Nolte, *Tetrahedron Lett*., 2002, **43**, 9351.
27 B. K. Roland, H. D. Selby, M. D. Carducci and Z. Zheng, *J. Am. Chem. Soc*., 2002, **124**, 3222.
28 K. Araki, C. A. Silva, H. E. Toma, L. H. Catalani, M. H. G. Medeiros and P. Di Mascio, *J. Inorg. Biochem*., 2000, **78**, 269.
29 L. Monsù Scolaro, C. Donato, M. Castriciano, A. Romeo and R. Romeo, *Inorg. Chim. Acta*, 2000, **300–302**, 978.
30 (*a*) E. Iengo, E. Zangrando and E. Alessio, *Eur. J. Inorg. Chem*., 2003, 2371; (*b*) E. Iengo, E. Zangrando, S. Geremia, R. Graff, B. Kieffer and E. Alessio, *Chem.-Eur. J*., 2002, **8**, 4670; (*c*) E. Alessio, E. Iengo and L. G. Marzilli, *Supramol. Chem*., 2002, **14**, 103; (*d*) E. Iengo, E. Zangrando, R. Minatel and E. Alessio, *J. Am. Chem. Soc*., 2002, **124**, 1003; (*e*) E. Iengo, B. Milani, E. Zangrando, S. Geremia and E. Alessio, *Angew. Chem., Int. Ed*., 2000, **39**, 1096.
31 (*a*) E. Zangrando, B. Serli, L. Yellowlees and E. Alessio, *Dalton Trans*., 2003, 4391; (*b*) B. Serli, E. Zangrando, T. Gianferrara, L. Yellowlees and E. Alessio, *Coord. Chem. Rev*., 2003, **245**, 75; (*c*) B. Serli, E. Zangrando, E. Iengo, G. Mestroni, L. Yellowlees and E. Alessio, *Inorg. Chem*., 2002, **41**, 4033.
32 (*a*) L. G. F. Lopes, A. Wieraszko, Y. El-Sherif and M. J. Clarke, *Inorg. Chim. Acta*, 2001, **312**, 15; (*b*) J. M. Slocik, M. S. Ward, K. V. Somayajula and R. E. Shepherd, *Transition Met. Chem*., 2001, **26**, 351; (*c*) D. R. Lang, J. A. Davis, L. G. F. Lopes, A. A. Ferro, L. C. G. Vasconcellos, D. W. Franco, E. Tfouni, A. Wieraszko and M. J. Clarke, *Inorg. Chem*., 2000, **39**, 2294; (*d*) J. M. Slocik and R. E. Shepherd, *Inorg. Chim. Acta*, 2000, **311**, 80; (*e*) S. da S. S. Borges, C. U. Davanzo, E. E. Castellano, J. Z-Schpector, S. C. Silva and D. W. Franco, *Inorg. Chem*., 1998, **37**, 2670; (*f*) P. C. Ford, J. Bourassa, K. Miranda, B. Lee, I. Lorkovic, S. Boggs, S. Kudo and L. Laverman, *Coord. Chem. Rev*., 1998 **171**, 185.
33 A. Gabrielsson, F. Hartl, J. R. Lindsay Smith and R. N. Perutz, *Chem. Commun*., 2002, 950.
34 P. J. Dyson and J. S. McIndoe, *Inorg. Chim. Acta*, 2003, **354**, 68.
35 Collaborative Computational Project Number 4, *Acta Crystallogr., Sect. D*, 1994, **50**, p. 760.
36 (*a*) G. M. Sheldrick, *SHELXS-97, Program for solution of crystal structures*, University of Göttingen, Germany, 1997; (*b*) G. M. Sheldrick, *SHELXL-97, Program for refinement of crystal structures*, University of Göttingen, Germany, 1997.
37 L. J. Farrugia, *J. Appl. Crystallogr*., 1999, **32**, 837.
38 B. Serli, E. Zangrando, E. Iengo and E. Alessio, *Inorg. Chim. Acta*, 2002, **339**, 265.
39 V. E. Yushmanov, H. Imasato, T. T. Tominaga and M. Tabak, *J. Inorg. Biochem*., 1996, **61**, 233.
40 R. Lauceri, R. Purrello, S. J. Shetty and M. G. H. Vicente, *J. Am. Chem. Soc*., 2001, **123**, 5835.
41 C. K. Johnson, *ORTEP* (Report ORNL-5138), Oak Ridge National Laboratory, Oak Ridge, TN, 1976.
42 W. I. White, in *The Porphyrins*, ed. D. Dolphin, Academic Press, New York, 1978, vol. 5, pp. 303–339.